Numerical Modeling of Subsurface Blasts

Jhon Silva Castro[1], L. Sebastian Bryson[2] (corresponding author), Nathan K. Gamber[3], Braden T. Lusk[4]
[1]*Research Assistant, Department of Mining Engineering – University of Kentucky, Lexington, KY, USA*
[2]*Assistant Professor, Department of Civil Engineering – University of Kentucky, Lexington, KY, USA, Email:* bryson@engr.uky.edu
[3]*Associate II, Wiss, Janney, Elstner Associates, Inc., Fairfax, VA, USA*
[4]*Assistant Professor, Department of Mining Engineering – University of Kentucky, Lexington,KY, USA*

ABSTRACT
When an explosion occurs on or below the ground surface, a phenomenon known as “ground shock” immediately follows. Ground shock is the propagation of compressive, shear, and tensile waves through earth media. Peak ground shock propagation in an earth medium is a complex function of the dynamic constitutive properties of the soil, the detonation products, and the geometry of the explosion. Due to the complexity of this type of problem, prediction of displacement and particle velocity and acceleration in the earth media resulting from a blast can be a very difficult task. The state-of-the-practice for describing and predicting these blast response parameters utilizes empirical formulas. These empirical formulas typically represent the earth medium as a homogeneous, isotropic mass and thus characterize the blast response within the medium using basic measures of linear elasticity. Unfortunately, natural earth deposits are seldomly isotropic, homogeneous masses and due to the large strains associated with a ground shock loading event, the dynamic response of the mass cannot be adequately described using linear elasticity.
This paper presents the results of a study that evaluated the performance of a finite element model developed to predict peak particle velocity and pressure for free-field blast conditions. The influences of domain size, boundary conditions and the damping coefficients on the model performance were analyzed and the results are presented. The results of the numerical model were compared against case histories where empirical equations and monograms were developed to relate dynamic properties of soils to ground shock predictions. Finally, the influence of the soil constitutive model used in the numerical model is presented.

RESUMEN
Cuando ocurre una explosión en la superficie o a una cierta profundidad del terreno, se genera un fenómeno conocido como un “impacto en el terreno”. El impacto en el terreno es la propagación de ondas compresivas, de corte y de tensión a través del terreno. El valor máximo o pico y su propagación es una función compleja que involucra las propiedades dinámicas y constitutivas del suelo, la composición química de los productos que detonan, y la geometría de la explosión. Debido a la complejidad de este problema, la predicción del desplazamiento, la velocidad y la aceleración del terreno en un lugar particular puede difícil. En la práctica, el estado del arte para describir y predecir los parámetros de respuesta del terreno debido a una voladura utiliza formulas empíricas. Esas formulas suponen el medio en donde se desarrolla el fenómeno como una masa homogénea, e isotrópica y caracteriza la respuesta en el medio usando elasticidad lineal. Desafortunadamente los depósitos térreos son raramente isotrópicos. Adicionalmente, debido alas grandes deformaciones producidas en una voladura, la respuesta dinámica del terreno no puede ser adecuadamente descrita usando elasticidad lineal. Este documento presenta los resultados de un estudio que evaluó la eficiencia de un modelo de elementos finitos para predecir la velocidad pico partícula y la presión del terreno para condiciones de campo libre. En el desarrollo del modelo, fueron analizadas la influencia del tamaño del dominio o el tamaño del modelo, las condiciones de frontera y finalmente los coeficientes de amortiguamiento utilizados. Los resultados de estos estudios paramétricos son presentados. Los resultados obtenidos fueron comparados contra casos históricos donde ecuaciones empíricas y monogramas fueron desarrollados para relacionar las propiedades dinámicas del suelo con las predicciones de la explosión. Finalmente, la influencia del modelo constitutivo del suelo en el modelo numérico es presentada.

1 INTRODUCTION

Infrastructure protection against blast events is important regardless if the source of the explosion is from a terrorist attack, mining activities or excavations due to civil works. Structures supported on shallow foundation systems, such as buildings, bridges, and power transmission towers are the most vulnerable to subsurface blasting loads.

There are different responses of foundation systems to a blast event. Such responses can range from instantaneous, severe damage or destruction, up to long-term geotechnical effects that generate differential settlements, footing rotations and ultimately bearing capacity failure.

There are several models and idealizations to explain what happens when a buried charge of explosives is detonated. In general, two zones are associated with blast phenomena; generation and seismic transmission zones (Enescu et al., 1973; Bollinger, 1980; Saharan et al., 2006). The generation zone is the area where the energy contained in the explosive chemical reaction is released. In this zone, tremendous pressure and high temperatures are developed due to the chemical reaction. As a result, the solid medium is subject to inelastic phenomena such as breaking, shearing and crushing of the soil particles. Also, large strains are developed within this zone. A discussion of the inelastic process within the generation zone in an explosion can be found in Cook (1958) or in Langefors and Kihlstrom (1963).

The seismic transmission zone is observed at some distance from the explosion where the inelastic phenomenon ends and the elastic behavior begins to govern the solid medium. Within the seismic transmission zone, the elastic disturbance propagates as seismic waves. In the transmission zone, the solid medium returns to its initial state after passage of the seismic disturbance.

The seismic waves propagating through the earth media can be divided in two major categories; body waves and surface waves. Body waves propagate through the solid medium (soil or rock) and surface waves travel along the surface. The main surface wave is the Rayleigh wave denoted by R-wave. Body waves can be subdivided into compressive waves, P-waves, and shear waves, S-waves.

Explosions produce mainly body waves (P and S) at small distances while R-waves become important at larger transmission distances (Dowding, 1985). The waveforms can be idealized for far and close distances according to the location of the recording site. The two idealized waveforms are explained using Figure 1. If the strain, pressure, or particle velocity, PV, is measured at Point A (close-in explosion), the shape of the idealized wave will be a single-spiked pulse. This is because at Point A only direct-transmission of the waves generated by the explosion is measured. On the other hand, if the recording site is located at Point B (far explosion), the idealized waveform of the strain, pressure or particle velocity will be more like a sinusoidal shape. At Point B the sinusoidal waveform will be a combination of direct-transmission, reflection and refraction waves.

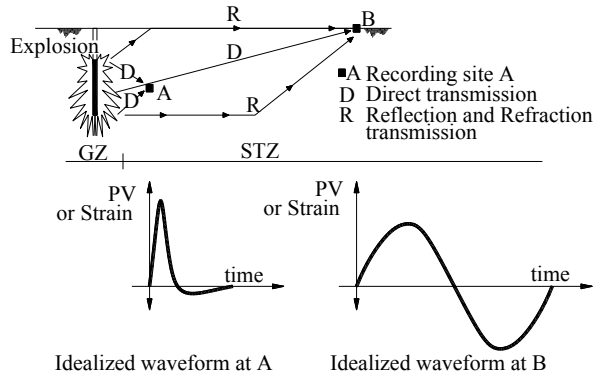

Figure 1. Waveform idealization in a blast event.

Prediction of particle displacement, velocity, acceleration, pressure and other parameters in the earth media resulting from an explosive detonation is a complicated and difficult task. Primary guidance on this topic is from the United States Department of the Army Technical Manual “Fundamentals of Protective Design for Conventional Weapons,” (TM-5-855-1, 1986). Other guidance is given by (Bulson, 1997). Both are generally complimentary to one another and are typically used together to predict blast response and blast–induced parameters. Although these documents are useful, they are limited to generic site and soil conditions. The desire is to be able to use a relatively simple numerical modeling package to model specific site and soil conditions.

This paper presents the results of a numerical model development using finite elements (FE) to evaluate ground response to blast loading. Specifically discussed in this paper is the numerical modeling of the behavior in a close-in explosion (Point A in Figure 1). Issues relating to the model development and calibration, the influence of domain size, the boundary conditions and the damping coefficients were analyzed and the results are presented. The calibrated model was used to compare some case histories and empirical equations that relate dynamic properties of soils to ground shock predictions.

2 FINITE ELEMENT MODEL DEVELOPMENT

2.1 Mesh Generation

The Plaxis 2D Dynamics Module, V8, FE code (Brinkgreve and Broere, 2002) was used to perform the simulations. The geometry was simulated by means of an axisymmetric model in which the blast crater was positioned along the axis of symmetry. The deformation and stress state are assumed to be identical in any radial direction. The axisymmetric model resulted in a 2D finite element model with two translation degrees of freedom per node.

Proper construction of the finite element mesh is necessary in order to accurately represent the behavior and response of a given problem. Plaxis has a built in finite element mesh generator. Element size is related to the accuracy of the predicted results. In areas where absolute representation of material behavior is necessary, a smaller element size is used. In addition, mesh refinement was used in the model the zone close to the explosive load application. The typical mesh configuration used for the models in the study is presented in Figure 2.

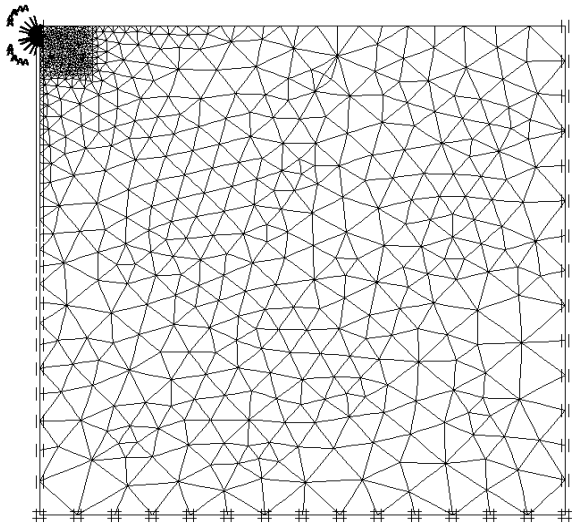

Figure 2. Mesh refinement.

2.2 Boundary Conditions

Plaxis provides built-in boundary conditions for use in a dynamic analysis. These boundary conditions are referred to as Standard Fixities and Standard Absorbent Boundaries. Standard Fixities imposes a set of general boundary conditions, which apply roller supports to the horizontal boundary sides of the model and fixed supports along the bottom vertical boundary of the model. An absorbent boundary is required to absorb the increments of stresses on the boundaries caused by dynamic loading that otherwise would be reflected inside the soil body. When performing a dynamic analysis in Plaxis, absorbent boundaries must be included. For an axisymmetric two-dimensional model, standard absorbent boundaries are generated at the bottom and right-hand boundaries of the model. The left-hand boundary is the axis of symmetry and the top boundary represents the ground surface. Therefore, absorbent boundaries are not applied to these two sides of the model. When performing a dynamic analysis, it is also important to choose a model size having dimensions a significant distance away from the vibration source. This helps to avoid unwanted and unrealistic reflection of ground shock waves (Yang, 1997).

Along with the absorbent boundaries, Plaxis provides relaxation coefficients *C1* and *C2*, which are used to help improve the wave absorption on the absorbent boundaries. Dissipation of waves in the direction normal to the boundary is corrected by *C1*, while *C2* corrects for wave dissipation in the tangential direction. The absorbent boundaries used in Plaxis are viscous boundaries, or dampers. Viscous boundaries are dash pots that dissipate the stress increase due to reflection at the boundaries. Plaxis defines the stress components in the dashpot as

$$\sigma = C1 \times \rho \times V_p \times V_x \quad [1]$$

$$\tau = C2 \times \rho \times V_s \times V_y \quad [2]$$

where σ = Normal stress; τ = Shear stress; ρ = Material density; V_p = Compressive wave velocity; V_s = Shear wave velocity; V_x = Horizontal velocity; V_y = Vertical velocity.

Plaxis recommends using values of *C1* = 1 and *C2* = 0.25 for all practical applications. These factors are based on a comparison of calculation results to theoretical formulas for a cantilever beam under dynamic load. In this paper, the best fit between calculation results and theoretical solutions was reached for *C1* = 1 and *C2* = 0.25.

3 CASE HISTORY

In order to verify that a blast simulation could be sufficiently modeled using Plaxis, two case histories for free-field blasting (i.e. no buried structures in the soil mass) were modeled. The two case studies are the Yang (1997) case history, which presents the results of an underground blast load and Rosengren et al. (1999) case history, which presents the results of a surface blast load. As part of the modeling process, the parameters of the finite element model were calibrated by performing a variety of parametric studies, the results of which are presented later. The calculation results of the Plaxis models were then compared to case history data and empirical relationships given by TM 5-855-1 (1986) for free-field pressures and ground motions.

3.1 Underground Blast Case History

Yang (1997) performed research using the commercial finite element software ABAQUS to predict the response of buried shelters to blast loadings. Part of the research involved a free-field analysis, which was investigated by using a 2-D finite element analysis in which a viscoelastic soil model was used. Yang (1997) then compared free-field pressures generated in the finite element analysis to those calculated from the empirical relationships given in TM 5-855-1 (1986). In the analysis, the detonation of the blast was represented by a pressure load that was applied to the circumference of a circle with a given radius, whose center coincided with that of the explosive charge. The pressure loading on the circumference of the circle was calculated using equations given in TM 5-855-1 (1986). Figure 3 shows the blast schematic used by Yang (1997) in order to build the numerical model.

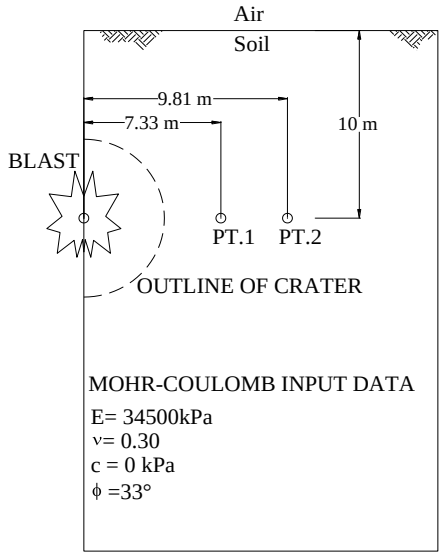

Figure 3. Underground blast schematic for numerical code (after Yang, 1997).

As shown in Figure 3, data was recorded at two points located at horizontal distances of 7.33 m and 9.81 m away from the blast detonation. The boundary was set at a sufficient distance away from the blast detonation to simulate an infinite boundary. The point under consideration for the calibration study is Point 1 (R = 7.33 m).

Yang (1997) chose a generic sand for the soil conditions and used the Mohr-Coulomb soil parameters as primary input into the viscoelastic soil model. The soil properties used in the Yang (1997) analysis are given in Table 1.

Table 1. Soil properties provided by Yang (1997).

Parameter		Definition	Value	Units
Soil	E	Modulus of elasticity	3.45E+04	kPa
	ν	Poisson's ratio	0.3	-
	ρ	Mass density	1.70E+03	kg/m^3
	ρ_c	Acoustic impedance	5.00E+05	Pa-sec/m
Dynamic Load	W	Charge weight	60	N
	H	Charge depth	10	m
	f	Ground shock coupling factor	1	-

3.2 Surface Blast Case History

Rosengren et al. (1999) performed a free-field analysis on a moraine soil, using the Mohr-Coulomb model. Using this case history allowed for a direct comparison with the results from the Yang (1997) case history. Soil and blast properties used by Rosengren et al. (1999) are presented in Table 2. Figure 4 shows the blast schematic used by to build the numerical model.

Table 2. Soil properties provided by Rosengren et al. (1999).

Parameter		Definition	Value	Units
Soil	E	Modulus of elasticity	88.8E+04	kPa
	ν	Poisson's ratio	0.4	-
	ρ	Mass density	1.90E+03	kg/m^3
	ρc	Acoustic impedance	1.90E+06	Pa-sec/m
Dynamic Load	W	Charge weight	245	N
	H	Charge depth	0.61	m
	f	Ground shock coupling factor	0.9	-

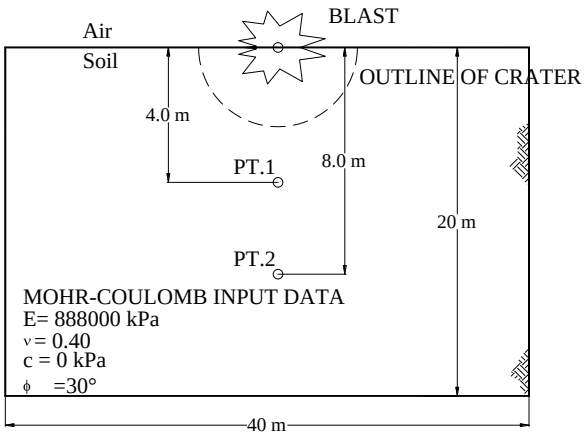

Figure 4. Surface blast schematic for numerical model (after Rosengren et al., 1999).

As shown in Figure 4, Rosengren et al. (1999) provided peak particle velocity data for two points located at vertical distances of 4.0 m and 8.0 m below the explosive charge.

4 MODEL CALIBRATIONS

4.1 Dynamic Load

The blast detonation was modeled in the same manner for both case histories. A dynamic load in the form of a uniformly distributed pressure load was applied to the boundary of the crater. The dynamic pressure load was made to increase instantaneously in magnitude to its peak value and then decay to zero after certain duration, corresponding to an ideal detonation (Aimone, 1992; Olsson et al., 2001). The dynamic pressure-time history load was input into Plaxis by means of a user-defined ASCII file. The pressure-time history load was calculated using equations given in TM 5–855-1 (1986) given by

$$P_0 = f \times \rho_c \times 160 \times \left(\frac{R}{W^{1/3}} \right)^{-n} \quad [3]$$

where P_o = Peak pressure (psi); f = coupling factor (f=1); ρ_c = acoustic impedance (psi/fps); R = distance to the explosion (ft); W = charge weight (lb).

Using Equation 3, peak pressures were found to be 10 MPa for the Yang (1997) case history and 20 MPa for the Rosengren et al. (1999) case history. Figure 5 shows the pressure-time histories used for the blast events in modeling the Yang (1997) and Rosengren et al. (1999) case histories.

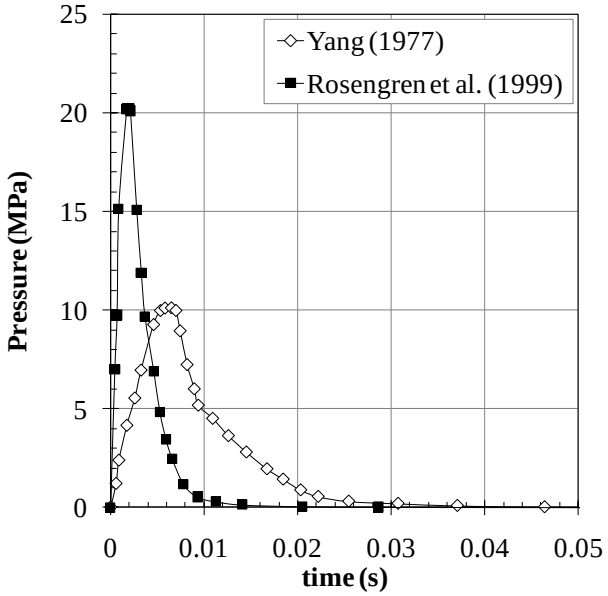

Figure 5. Pressure-Time histories.

4.2 Domain Size

The model calibration also included choosing an appropriate domain for the finite element model. The intent was to set the boundary at a sufficient distance away from the blast detonation to simulate an infinite boundary. The point under consideration for the calibration study is Point 1 (R = 7.33 m) in the Yang (1997) case history (see Figure 3). Figure 6 shows the effects of the model domain size on peak particle velocity. It can be seen that as the model domain increase, the peak particle velocities decreased and became closer to the empirical value.

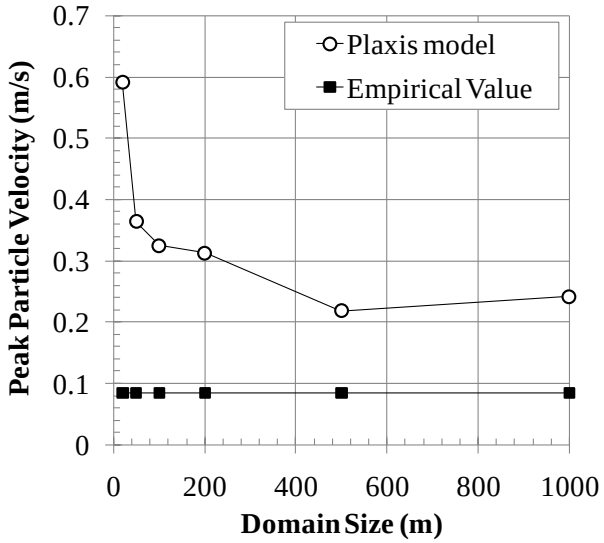

Figure 6. Peak particle velocity convergence analysis.

As shown in Figure 6, a domain size of 500 × 500 m was appropriate for the present analysis. Figure 7 shows the complete waveform for the absolute value of particle velocity versus time in seconds for the domain of 500 × 500 m and 200 × 200 m. The empirical prediction for this point is also included.

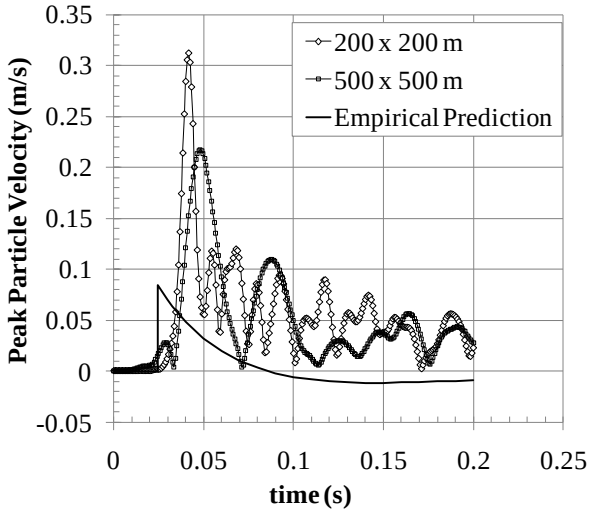

Figure 7. Peak particle velocity versus time.

4.3 Material Damping

By studying Figure 7, it can be seen that a substantial amount of wave reflection is occurring over time in both models. The smooth exponential decay and the peak value as predicted by the empirical equation are not evident. It is apparent that the peak particle velocity decreased as the domain size increased. However, increasing the model domain did not seem to dampen out the noticeable wave reflection. This wave reflection was due to the lack of material damping in the system.

In soils, damping is mainly due to loss of energy resulting from internal friction in the material and viscous

properties. A damping term know as Rayleigh damping can be determined to account for natural damping and was used in the finite element analysis for this research. The basic equation of motion of a body under the influence of a dynamic load is,

$$[M]\{\ddot{u}\} + [C]\{\dot{u}\} + [K]\{u\} = \{F\} \quad [4]$$

where [M] = Mass matrix; [C] = Damping matrix; [K] = Stiffness matrix; $\{\ddot{u}\}$ = Acceleration vector; $\{\dot{u}\}$ = Velocity vector; $\{u\}$ = Displacement vector; {F} = Load vector.

The matrix C represents the material damping of the materials. In reality, material damping is caused by friction or irreversible deformations (plasticity or viscosity). By increasing viscosity or plasticity, more vibration energy can be dissipated. If elasticity is assumed, damping can still be taken into account using the damping matrix C. However, other parameters are necessary in order to determine the damping matrix. In finite element formulations, the matrix C is often formulated as a function of the mass and stiffness matrices, and is known as Rayleigh damping. The damping matrix is then given as,

$$[C] = \alpha [M] + \beta [K] \quad [5]$$

where α, β = Rayleigh damping coefficients.

The Rayleigh damping coefficients are used to determine the damping matrix. However, the Rayleigh damping coefficients are difficult to establish. The α and β coefficients are determined from damping ratios that correspond to natural frequencies of vibration. The relationship between these parameters is given by,

$$\alpha + \beta\omega^2 = 2\omega\varsigma \quad [6]$$

where ς = Damping ratio; ω = Natural frequency of vibration. The damping ratios and natural frequencies can be determined experimentally by using tests such as the resonant column test performed on the given material.

Unfortunately, advanced testing was not performed on the case history soils .Thus, the best possible fit for the Rayleigh α and β was determined by a trial and error calibration method. This was done by holding the α value constant for three different values of β and then varying the β value over a given range. The results of this exercise are shown in Figure 8.

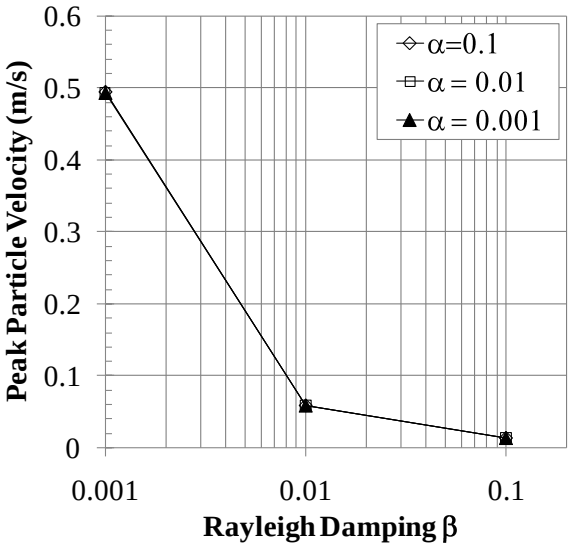

Figure 8. Peak particle velocity as a function of Rayleigh damping parameters.

It can be seen from Figure 8 that there is little to no difference when the α value is changed. Hence, the best fit for the empirical value of peak particle velocity occurred at α = 0.001 and β = 0.01, which corresponds with a PPV close to the reference value.

By introducing damping into the system, the decay of the particle velocity curve is a better match to the empirical relationship. Figure 9 demonstrates the absence of wave reflection and the smoother decay of the curve from the peak value. This figure reflects a mesh configuration with no refinement around the charge.

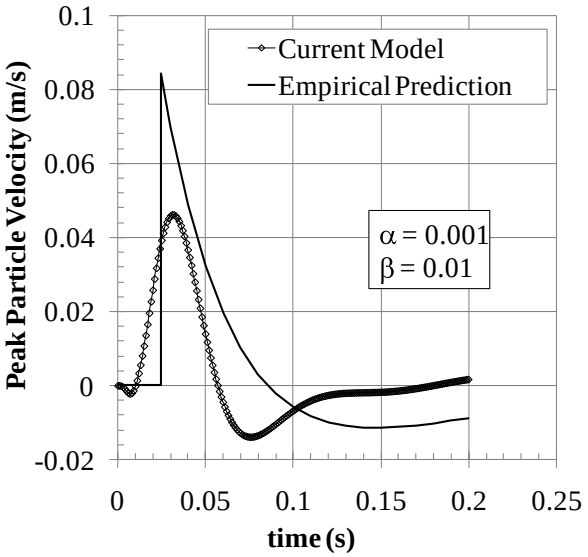

Figure 9. Peak particle velocity versus time with Rayleigh damping.

Yang (1997) compared results of the viscoelastic soil model with damping to two seismic velocity values. One value was 165 m/s, calculated directly from the elastic constants of the soil, while the other was 300 m/s, a value

given in TM 5-855-1 (1986) and commonly used for soils. Yang (1997) noted that for the viscoelastic model, the finite element results correspond to the seismic velocity of 300 m/s. It was concluded that seismic velocity calculation directly from the elastic properties of a given soil is not the most accurate method. That calculation can be used as an acceptable estimate, but may not be consistent with the field conditions. The current paper shows similar results with regards to the seismic velocity for the Mohr-Coulomb model. The 300 m/s value was used to calculate the empirical response in this paper.

5 ANALYSIS OF RESULTS

Upon completion of the model calibration, the best possible model parameters were chosen for modeling the Yang (1997) case history. The results of the current model versus the empirical approach for the Points 1 and 2 are presented in Figure 10.

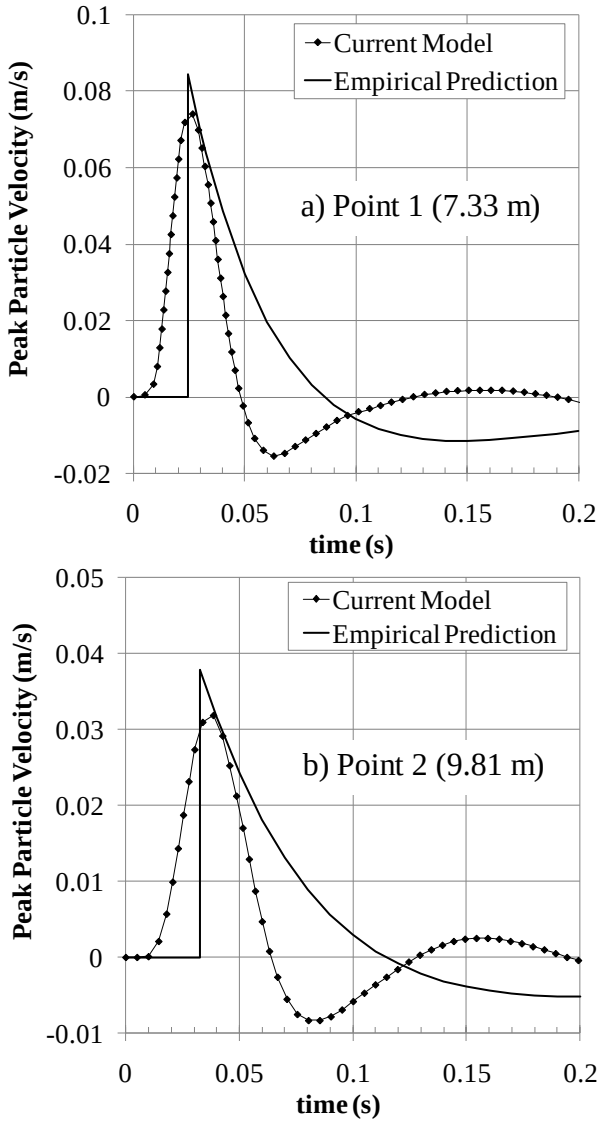

Figure 10. Peak particle velocity versus time comparison.

Figure 10 reflects a mesh configuration with refinement around the charge. Figure 10 shows that the Plaxis model was able to match the empirical equations presented in TM 5-855-1 (1986) fairly well by matching the peak particle velocity values and arrival times.

Yang (1997) originally compared pressure in Points 1 and 2 rather than particle velocity. Due to this, Figure 11 shows the pressure versus time for the Points 1 and 2.

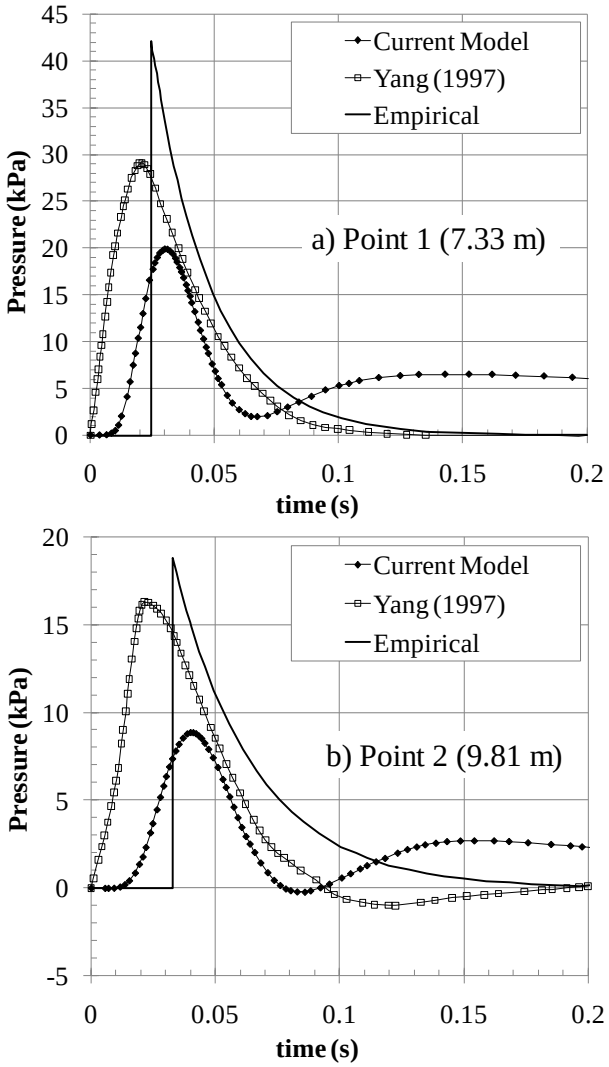

Figure 11. Pressure versus time comparison.

In this case, the Plaxis model performance was “fair” relative to the free-field analysis performed by Yang (1997).

Figure 12 presents the peak particle velocity as a function of time for the Rosengren et al. (1999) case history. It should be noted it was assumed that the same parameters such as domain size, Rayleigh damping coefficients, mesh coarseness and mesh refinement previously determined for the calibration of the Yang (1997) case history were adopted for modeling the Rosengren et al. (1999) case history. As can be seen in the figure, the Plaxis model appears to capture the blast behavior well.

From Figures 10 to 12, it can be seen that the results obtained from the Plaxis analysis are in agreement with the results presented by Yang (1997), and Rosengren et al. (1999). This result establishes that blast events can be reasonably modeled in Plaxis using a Mohr-Coulomb soil model.

Analysis using the Hardening-Soil model (Schanz et al., 1999) was performed as an investigation into whether or not the use of a more advanced soil model would yield results that were noticeably more accurate than those of the Mohr-Coulomb model. Unfortunately, the results from that analysis were inconclusive. Thus, it was determined that the Mohr-Coulomb soil model and the parameters used sufficiently reflected soil behavior for the purposes of this paper.

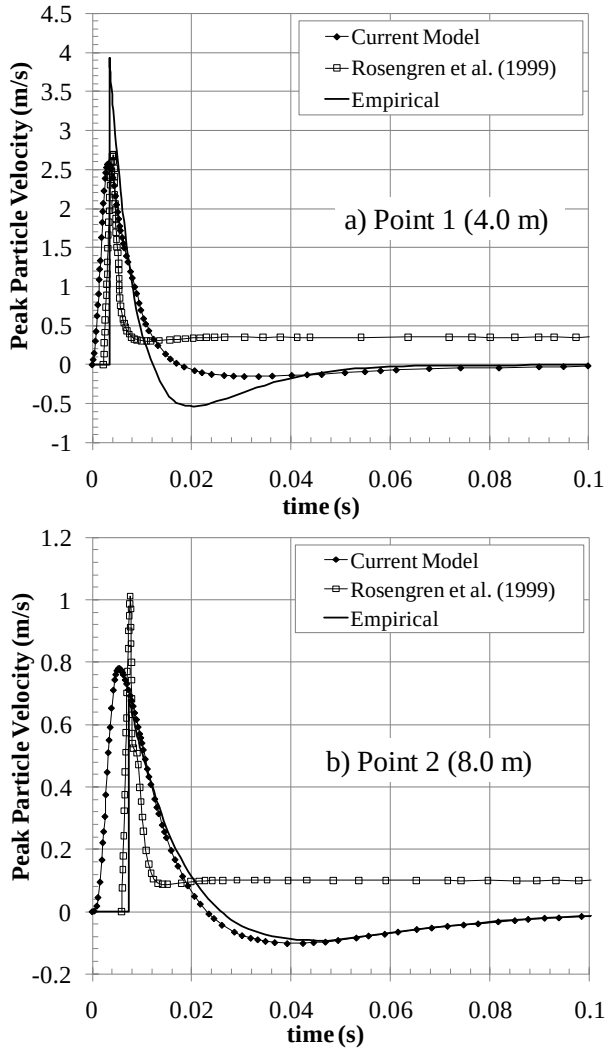

Figure 12. Peak particle velocity versus time comparison.

6 CONCLUSIONS

It was determined that Plaxis software is capable of modeling blast events and provides a useful tool for blast prediction purposes. Two case histories were modeled and yielded acceptable results.

Plaxis results compared well to results provided by the case histories and to empirical relationships provided by TM 5-855-1 (1986).

7 ACKNOWLEDGEMENTS

The material presented in this paper is based upon work supported by the Ohio University Stocker Endowment Research Fund and funds provided by the Kentucky Office of Surface Mining. Without this financial support, this work would not have been possible.

8 REFERENCES

Aimone, C. T. (1992) “Rock breakage: Explosives, blast design.” *SME Mining Engineering Handbook*, H.L, Hartman, ed. Society of Mining Engineers, Littleton, CO, 722-746

Bollinger, G.A. (1980). *Blast Vibration Analysis*, Southern Illinois University Press, Carbondale, IL 132 pp.

Brinkgreve, R. B. J. and Broere, W. (2002). “Geotechnical Code for Soil and Rock Analysis.” *Plaxis, 2D, Version 8 Users Manual*, A.A. Balkema Publishers, Netherlands.

Bulson, P.S. (1997). *Explosive Loading of Engineering Structures*, 1st ed., E & FN Spon Publishers, New York, NY, 236 pp.

Cook, M.A. (1958). *The Science of High Explosives*, American Chemical Society, Monograph No. 136, 440 pp.

Dowding, C.H. (1985). *Blast Vibration Monitoring and Control*, Prentice Hall, Englewood Cliffs, NJ., 297 pp.

Enescu, D., Geogescu, A. and Marza, V. (1973). “Simulations of the underground explosions generating longitudinal and transverse waves.” Bulletin of the Seismological Society of America, 63(3), 753-763.

Langefors, U. and Kihlstrom, B. (1963). *The Modern Technique of Rock Blasting*, John Wiley & Sons, New York, NY.

Olsson, M., Nie, S., Bergqvist, I., and Ouchterlony, F. (2001). “What causes cracks in rock blasting?” *Proceedings of. EXPLO2001*. Hunter Valley, NSW, Australia, 191-196.

Rosengren, L., Olofsson, S.O., and Svedbjork, G. (1999). “Modeling of Ground-Shock Wave Propagation in Soil Using FLAC.” *Flac and Numerical Modeling in Geomechanics*, Detournay and Hart ed., A.A Balkema Publishers, Rotterdam, Netherlands, pp. 401-405.

Saharan, M.R., Mitri, H.S. and Jethwa, J.L. (2006). “Rock fracturing by explosive energy: review of state-of-the-art,” *Fragblast*, 10(1), 61-81.

Siskind, D.E., and Stagg, M.S. (1985). “Blast Vibration Measurements Near and On Structure Foundations.”

Report of Investigation 8969, U.S. Bureau of Mines, Washington, DC, 20 pp.

Siskind, D.E., Dowding, C. H., Kopp, J.W., and Stagg, M.S. (1980). “Structure Response and Damage Produced by Ground Vibration From Surface Mine Blasting.” *Report of Investigation 8507,* U.S. Bureau of Mines, Washington, DC, 74 pp.

TM 5-855-1 (1986). “Fundamentals of Protective Design for Conventional Weapons,” *Technical Manual 5-855-1*, U.S. Department of the Army, Headquarters, Washington, DC.

Yang, Z. (1997). “Finite Element Simulation of Response of Buried Shelters to Blast Loadings.” *Finite Elements in Analysis and Design*, 24(3), 113-132.